Acta Crystallographica Section D
Biological Crystallography
ISSN 0907-4449

Ab initio crystallographic structure determination of insulin from protein to electron density without crystal handling

José A. Gavira,[a] Diana Toh,[a] Javier Lopéz-Jaramillo,[b] Juan M. García-Ruíz[b] and Joseph D. Ng[a]*

[a]Laboratory for Structural Biology and the Department of Biological Sciences, University of Alabama in Huntsville, Huntsville, AL 35899, USA, and [b]Laboratorio de Estudios Cristalograficos, IACT CSIC-UGRA, Facultad de Ciencias, Granada 18002, Spain

Correspondence e-mail: ngj@email.uah.edu

Received 28 November 2001
Accepted 17 April 2002

Insulin crystals suitable for cryogenic data collection and structure determination by single-wavelength anomalous scattering (SAS) were obtained by a self-optimization screening process in a single capillary tube without manipulation of the crystals at any time. Using the counter-diffusion crystallization technique, screening for optimal conditions for crystal growth, incorporation of a strong anomalous scattering halide and cryogenic solution took place simultaneously in a single capillary tube. The crystals in the capillaries can be placed directly in the cryostream for data collection using a conventional home-laboratory X-ray source. High-redundancy data were used to obtain a Patterson solution from the anomalous signal of iodine. As a result, the anomalous scattering-atom position was determined and the phase calculated, giving rise to an initial electron-density map at 2.4 Å resolution. This entire procedure from crystal growth to the determination of an initial structure was performed within four weeks.

1. Introduction

Ab initio protein structure determination by X-ray crystallography without any *a priori* structural information relies on several critical steps. The first and inevitably the bottleneck step is to obtain crystals suitable for X-ray diffraction. Crystallization generally requires a significant quantity of a pure protein sample to undergo exhaustive crystallization screens, typically with different types of precipitating agents and a pH and temperature range (McPherson, 1999; Ducruix & Giegé, 1999). After initial crystallization conditions are found, further screens must be performed to optimize the conditions for crystal growth. In this case, the crystallization preparation is usually adjusted such that the initial supersaturation and rate of equilibrium are refined to obtain the best quality crystals for X-ray diffraction analysis. Most protein crystals are very sensitive and will not survive long X-ray radiation exposure. The second step is to find cryoprotectant solutions to treat the protein crystals such that they can tolerate supercooling while sustaining their ability to diffract X-rays. Further screening is imposed on the crystallographer to systematically try a series of cryogenic solutions at different concentrations and soak times. The third step is to find a strong scattering atom either intrinsic to the protein (such as sulfur or metal ions) or as an incorporated derivative (such as halides or heavy metals) for *ab initio* phasing (Blundell & Johnson, 1976). Successful phase determination strongly depends on how intensely the derivatized atom scatters X-rays and on knowing precisely where in the crystallographic unit cell the atom is located. To find a suitable strong scattering-atom derivative requires yet another

rigorous search which is often exhaustive and labor intensive. The screening process examines different heavy atoms and conditions that will not disrupt the diffraction quality of the native crystal but will at the same time serve as a suitable scatterer for phase determination. This is the rate-determining step in the computational component of protein structure solution, since accurate phase determination using single isomorphous replacement (SIR; Green *et al.*, 1954), multiple isomorphous replacement (MIR; Harker, 1956), multi-wavelength anomalous scattering (MAD; Hendrickson, 1985), single anomalous dispersion (SAD; Hendrickson & Teeter, 1981; Smith & Hendrickson, 1983) or single-wavelength anomalous scattering (SAS; Wang, 1985; Chen *et al.*, 1991) require protein crystals with an adequate incorporation or derivatization of strongly scattering atoms.

It is clear that given a target protein much effort and time must be invested in the search for optimal conditions for crystal growth, cryopreservation, strongly scattering atom derivatization and data collection during the initial course of structure determination. This task becomes much more difficult when it involves simultaneously crystallizating many proteins and finding suitable conditions for efficient and accurate *ab initio* structure determination. This case comes to mind during the high-throughput protein structure determination programs associated with genomic projects. Despite the development of sophisticated tools and robotic systems for handling protein crystals in large-scale screens, there has not been any methodology developed to concurrently screen for suitable crystallization conditions, cryopreservatives and strongly scattering atom derivatives.

We report here an easy technique for the growth of optimal protein crystals from known crystallization conditions for direct X-ray data collection and structure determination. The crystal-growth conditions used to obtain the cubic crystalline form of insulin (Harding *et al.*, 1966) were used to optimize crystal growth by the restricted-geometry counter-diffusion technique described previously (García-Ruiz, 1991; García-Ruiz *et al.*, 1998) followed by cryogenic preservative treatment in the same crystallization container (Lopéz-Jaramillo, García-Ruiz *et al.*, 2001). The diffuse soaking of an anamolous scattering halide is performed concurrently during the crystal-optimization process; X-ray data collection and *ab initio* phasing were subsequently performed without crystal handling in any of the steps. We demonstrate this technique by showing the possibility of solving the structure of insulin without the use of any *a priori* structural information from crystal growth to the first initial electron-density map using a laboratory X-ray source.

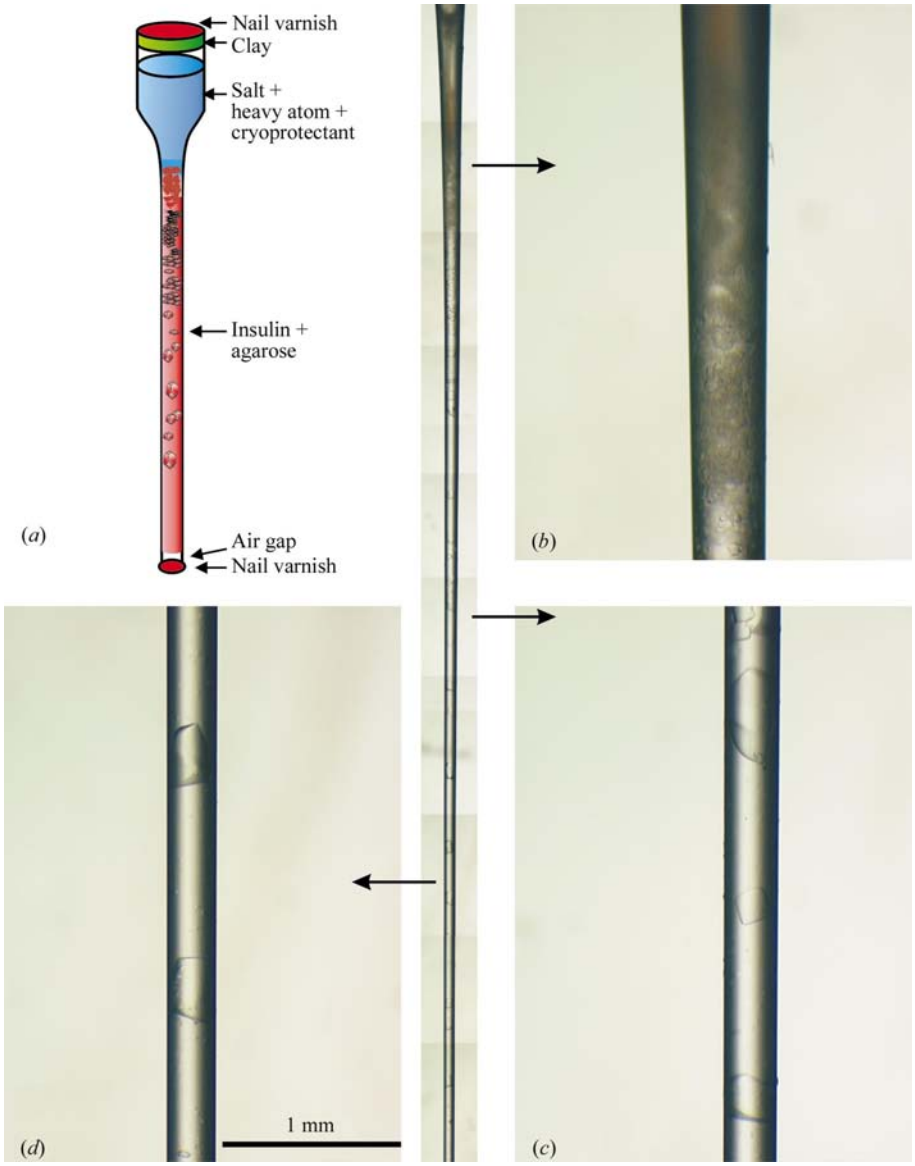

Figure 1
Counter-diffusion crystallization setup in an X-ray quartz capillary. In each experiment, two solution chambers are arranged adjoining one another. The first chamber contains the precipitating agent, anomalous scattering atom and cryopreservative. The second chamber holds the protein solution. The capillary is sealed with nail varnish and clay (*a*, adapted from López-Jaramillo, García-Ruiz *et al.*, 2001). During the course of the experiment, the salt solutions will initially diffuse into the protein layer, followed by the slower diffusing cryoprotectant reagent. Crystals appear across the capillary in a self-forming supersaturation gradient followed by slow incorporation of the cryoprotecting solution. The center capillary picture shows the consequence of a supersaturation wave, giving rise to an amorphous precipitate at the initial end (magnified in *b*) and separate crystals growing over the length of the capillary (magnified in *c* and *d*).

2. Materials and methods

2.1. Proteins and chemicals

Purified bovine pancreatic insulin (Cat. No. I5500, Lot 90K1933, Sigma, St Louis, MO, USA) was used throughout the experiment without further purification. Lyophilized insulin was dissolved in 0.1 *M* Tris–HCl and adjusted to pH 9.0 with 1 *M* NaOH. All solutions were made up with ultrapure water. Protein concentration was calculated from the absorbance at 280 nm using a molar extinction coefficient of 0.83 cm^{-1} ml mg^{-1} (Fasman, 1989). The agarose used was purchased from FisherBiotech (Cat. No. BP 1356-100, Lot No. 006896).

2.2. Crystallization

The crystallization of insulin was prepared in 0.3 mm quartz capillary tubes (Charles Supper Company, Natick, MA, USA) using the counter-diffusion method geometry (García-Ruiz, 1991). The protein sample was prepared by mixing 30–50 mg ml^{-1} insulin with 0.5% agarose solution in 100 m*M* Tris–HCl pH 9.0 in a volume ratio of 9:1. Approximately 10 µl of the resulting protein preparation was taken up into the narrow portion of the capillary by capillary action. The initial composition of the salt-chamber solution consisted of 13.5% sodium potassium phosphate as the precipitating salt (Harding *et al.*, 1966), 90 m*M* KI as the heavy-atom component and 22.7% glycerol as the cryogenic preservative. The mixture was layered carefully on the surface of the protein solution, forming a liquid–liquid interface. The ends of the capillary tube were sealed with nail varnish and clay. The final setup is illustrated in Fig. 1(*a*) and was placed horizontally in an incubator at 293 K. Crystals can be observed in as little as 3 d. However, the equilibrium of the cryogenic preservative is only reached after three weeks (López-Jaramillo, García-Ruiz *et al.*, 2001).

Agarose was incorporated at low concentration into the crystallization mixture to (i) decrease the convective mass transport of the environment (García-Ruiz *et al.*, 2001), (ii) avoid crystal slipping during the initial quality screening (Gavira, 2000; López-Jaramillo, García-Ruiz*et al.*, 2001) and (iii) increase the nucleation rate (Vidal *et al.*, 1998). The addition of agarose improves the self-optimizing crystallization process in the capillary and facilitates any subsequent transport demands (such as to a synchrotron source). While agarose is helpful in this crystallization procedure, it is not a critical component and can be omitted without disrupting the optimization process.

2.3. Crystal screening and data collection

The quality of crystals grown in the capillary was evaluated by visual inspection and X-ray diffraction analysis after as little as one week of equilibration. The crystals were observed through a polarized filter under a Nikon visible-light microscope and photographed with a Kodak Digital Science DC120 camera. The entire capillary containing the crystals was mounted vertically on an XYZ short standard goniometer head for X-ray analysis. Diffraction data were collected on capillary-mounted crystals using an MSC R-AXIS IV image-plate detector with a crystal-to-detector distance of 250 mm. The X-rays were generated by a Rigaku rotating-anode generator operated at 50 kV and 100 mA and focused with MSC OSMIC confocal mirrors. Images were collected at 1.0° oscillation angles with an exposure time of 15 min.

Initially, a single diffraction image was recorded at room temperature for each crystal in the capillary in order to determine which crystal yielded the best diffraction quality based on the resolution limit, the intensity of reflections over the background signal and the mosaicity of the reflection spots based on visual inspection. High-redundancy data collection was carried out from the best single crystal in the capillary tube. The capillary region containing the selected crystal was cut and glued against a Copper CrystalCap (Hampton Research, Laguna Niguel, CA, USA) and immediately flash-cooled in a nitrogen stream at 100 K using an MSC X-Stream Cryogenic Crystal Cooler System (Molecular Structure Corporation, The Woodlands, Texas, USA). These data were indexed using *DENZO* and reduced using *SCALEPACK* from the *HKL*2000 program package (Otwinowski & Minor, 1997).

2.4. Phasing and initial electron-density map calculations

The location of the I atoms was determined and refined with a data set truncated at 4.0 Å using *XTALVIEW* (McRee, 1999) and *PHASES* (Furey & Swaminathan, 1997). *CCP*4 programs (Collaborative Computational Project, Number 4, 1994) were used to calculate an anomalous difference Fourier map. The positions of the anomalous scattering atoms were determined and refined with *PHASES*. The program *ISAS* (Wang, 1985) was employed to calculate the phases and subsequently the initial $F_o \times$ f.o.m. map in a one-step iterative procedure. The initial insulin model and maps were visualized using *O* (Kleywegt & Jones, 1997) and *XTALVIEW*.

3. Results and discussion

3.1. Concurrent *in situ* optimization for crystallization, cryoprotectant and strongly scattering atom incorporation in capillary

Insulin was used as a model protein to demonstrate the feasibility of optimizing crystallization conditions in a counter-diffusion geometry against a precipitating salt (García-Ruiz, 1991; García-Ruiz & Moreno, 1994, 1997) while at the same time incorporating a cryoprotectant and a strongly X-ray scattering atom. X-ray capillaries have been well demonstrated to act as crystallization vessels where crystals can be grown *in situ* from a protein solution, cryoprotected and mounted on a flash-cooling stage at 100 K for successful X-ray data collection without any post-crystallization manipulation (López-Jaramillo, García-Ruiz *et al.*, 2001). Our study here extends this application to perform *in situ* screening of heavy-atom derivatives and shows the feasibility of solving the three-

dimensional structure of a protein quickly, efficiently and accurately from *ab initio* phasing.

Insulin has been crystallized in a cubic space group and its structure has been solved to 2.0 Å (Dodson *et al.*, 1978). Fig. 1 illustrates the pre-crystallization setup, where the lower narrow chamber is filled with protein and the upper chamber contains the precipitating agent, cryoprotectant and a halide salt.

Halide ions in crystallization media have been observed to occupy ordered positions by co-crystallization (Chen *et al.*, 1991, Lim *et al.*, 1998) or by fast-soaking methods (Dauter & Dauter, 1999; Dauter *et al.*, 2000, 2001) in protein crystals. The halide ions' anomalous scattering signals were strong enough to phase the protein structures. In light of this, we have used iodine or bromide salts as part of our precipitating solution mixture such that the halides can be incorporated into the capillary-optimization procedure. Iodine was found to provide the best results, producing adequate anomalous signals using a home X-ray source.

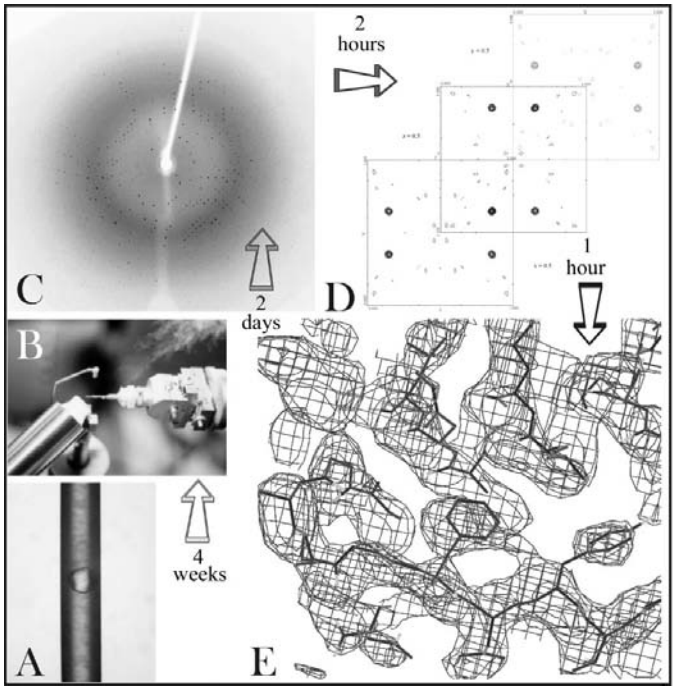

Figure 2
Process from crystal screening to an initial experimental structure model as a function of time. Insulin crystals derivatized with iodine, cryoprotected and determined suitable for X-ray analysis can be obtained within two to four weeks. Panel A shows a well isolated crystal in the length of the capillary (with a diameter of 0.3 mm) adequate for preliminary X-ray analysis at room temperature. The region containing the optimal crystal for X-ray diffraction was excized very carefully with a sharp glass cutter without shattering the capillary or damaging the crystals. The truncated capillary containing the selected crystals was mounted on a goniometer and flash-cooled immediately in a cryogenic stream at 100 K (panel B). Panel C shows a typical 1° oscillation diffraction photograph, with the outer radius being 2 Å resolution. Even though there is a notable diffuse background, the diffraction spots are very distinct and can be processed very easily. The most striking feature is the absence of any ice rings. Data collection at the home-laboratory source usually requires 2 d to obtain a high-redundancy data set. After data indexing and reduction, an anomalous difference Patterson map can be calculated identifying the iodine anomalous signals. The analysis of the complete data set to obtaining readable anomalous difference Patterson maps requires no more than a couple of hours. Panel D shows the anomalous peaks on the Harker sections contoured from 3σ to 11σ in 1σ increments. Finally, the positions of the I atoms can be located and the initial image of the protein can be obtained using the anomalous scattering signal of iodine followed by solvent flattening by the *ISAS* procedure within 1 h. Panel E illustrates the experimental electron-density map traced by the initial model of insulin.

Glycerol was chosen as the cryoprotectant since it is most commonly used for cryocrystallography (Garman & Schneider, 1997). Even though glycerol is not particularly encouraged for use as an additive in crystallization solutions owing to its potential to inhibit crystal nucleation and growth (McPherson, 1999), the current setup allows the nucleation, crystallization and glycerol treatment to occur in sequential events. When the precipitating salt mixture is in contact with the protein chamber, a liquid–liquid free-diffusion system is formed, activating a supersaturation wave along the protein chamber (García-Ruiz, Otálora *et al.*, 2001). This is a result of the salts initially diffusing into the protein solution, forming a salt gradient of high concentration near the protein-precipitating solution interface and falling to a lower concentration as it moves further across the capillary.

After one week of equilibration, single cubic crystals can be readily observed along the capillary (Figs. 1*b*–1*d*). The crystals are sufficiently cryoprotected only after three more weeks of equilibration. The crystals grown in the capillary range from 0.05 to 0.50 mm in the longest dimension, where the largest crystals fill the diameter of the capillary (Figs. 1*c* and 1*d*). Single crystals were screened for diffraction quality at room temperature. When the crystals along the length of the capillary were analyzed, they were not of equivalent quality: they diffracted X-rays to different limits and displayed varying intensity-to-noise ratios and mosaicity. Only optimal crystals identified were immediately used for X-ray data collection.

There are distinct advantages of growing crystals by the procedure described in this study compared with protein crystals obtained by conventional methods. In capillaries with diameters less or equal to 0.5 mm, the mass transport of the precipitant, halide and cryoprotectant is diffusion controlled. The crystals obtained in this stable environment are never exposed to drastic chemical changes that can potentially decrease crystal quality. Conventional methods require the physical transfer of protein crystals to solutions containing different metals or cryogenic preserving solutions prior to X-ray analysis. Crystals grown in capillaries, however, do not have to be removed from the mother liquor and subjected to different soaking environments. Thus, the capillary-grown crystals undergo minimal tension caused by osmotic (López-Jaramillo, Moraleda *et al.*, 2001) or mechanical stress that may lead to crystal cracking or dissolution.

3.2. Data collection and quality

The entire capillary can be mounted on any conventional goniometer and flash-cooled in the presence of a cryostream at 100 K. However, only a region of approximately 1 cm of the capillary can be efficiently frozen in the cryostream. Crystals

Table 1
Data-processing statistics.

Wavelength (Å)	1.54
Space group	$I2_13$
Unit-cell parameter a (Å)	78.14
Resolution range (Å)	25–2.4
No. of observations	50086
No. of unique reflections	3217
Redundancy	15.6
Crystal mosaicity† (°)	0.2
Completeness (%)	
Overall	99.8
Lowest shell (25–5.16 Å)	98.3
Highest shell (2.49–2.4 Å)	100.0
$R_{\rm merge}$‡ (%)	
Overall	11.2
Lowest shell (25–5.16 Å)	6.4
Highest shell (2.49–2.4 Å)	24.0
$I/\sigma(I)$	
Overall	28.1
Lowest shell (25–5.16 Å)	36.9
Highest shell (2.49–2.4 Å)	13.4

† Crystal mosaicity is defined, as in *DENZO*, as the rocking angle in degrees in both the vertical and the horizontal directions which would generate all the spots seen on a still diffraction photograph. ‡ $R_{\rm merge} = \sum_{hkl}\sum_i |\langle I\rangle - I_i|/\sum_{hkl}\sum_i I_i$.

located in juxtaposition to this region are damaged owing to the temperature gradient and ice formation, as determined by single X-ray diffraction images. In addition, the capillary can sometimes vibrate during data collection owing to the flow of the cryostream. If the capillary tube cannot be stabilized by mechanical means, it is sometimes necessary to truncate the length of the capillary and examine only a short region containing the target crystals. The resulting modification can be mounted onto a cryocap and flash-cooled into the cryostream (Fig. 2). However, it should be feasible to analyze the crystals in the entire capillary by maximizing the cryostream flow rate and adjusting the cold head nozzle to a broader cold flow.

A complete data set was recorded from a single crystal with over 15.6-fold redundancy, giving rise to excellent data-collection statistics (Table 1). The rotation range was selected to yield highly redundant anomalous data without employing an inverse-beam technique. The quality of the diffraction data was better than those observed from a single insulin crystal grown from a hanging drop using the same initial conditions, treated in a glycerol solution and fast soaked with KI (data not shown). Fig. 2 displays a typical diffraction image of the frozen insulin crystal screened in a capillary. There is no ice-ring formation or other aberrations. The reflection spots in the resolution range analyzed were fine, with a very low mosaic spread (see Table 1). There is slightly more background noise in the diffraction images from crystals grown in the capillary compared with that collected in a cryoloop owing to the glass and the excess solution. Nonetheless, the reflections were easily indexed and reduced.

3.3. Identification of anomalous sites

Bijvoet difference Patterson maps were calculated using the complete insulin data set from capillary-grown crystals to identify the largest anomalous signal. This map, shown in Fig. 2, had four large peaks, one of which is unique, on the Harker section at $z = 0.5$. The peaks were contoured starting from 3.0σ and in increments of 1.0σ for the observed Pattersons. Two main peaks were observed, refined and tested using the prediction algorithm of *XTALVIEW*. In a second procedure, *PHASES* was used to calculate and refine the position of the first iodine. From this, an anomalous difference Fourier electron-density map was calculated using the *CCP*4 suite (Fig. 3). This map displayed four other peaks, one of them identified as the density for the second I atom, already detected with *XTALVIEW* but not used during the phase calculation. The other three peaks were identified as being the three sulfur bridges present in insulin, showing high occupancy values after positional and occupancy refinement. Only the halide sites corresponding to peaks higher than 4σ in the anomalous difference map were used for the final phase determination.

3.4. *Ab initio* phase determination and initial electron-density map calculation

Only the iodine positions were used to determine the phases with an iterative algorithm to extract phases from intensity information of single-wavelength anomalous scattering data (*ISAS*; Wang, 1985). This procedure was originally used to calculate the image of the protein neurophysin II dipeptide complex at 2.8 Å from a single iodinated derivative (Chen *et al.*, 1991). More recently, the structure of the protein obelin has been solved using the anomalous scattering signal of sulfur to first estimate the image of the protein without using the image of the sulfur substructure in the crystal (Liu *et al.*, 2000). In our case, the *ISAS* procedure was performed in seven steps as described by Wang (1985) and Liu *et al.* (2000) to estimate the image of the protein using the anomalous

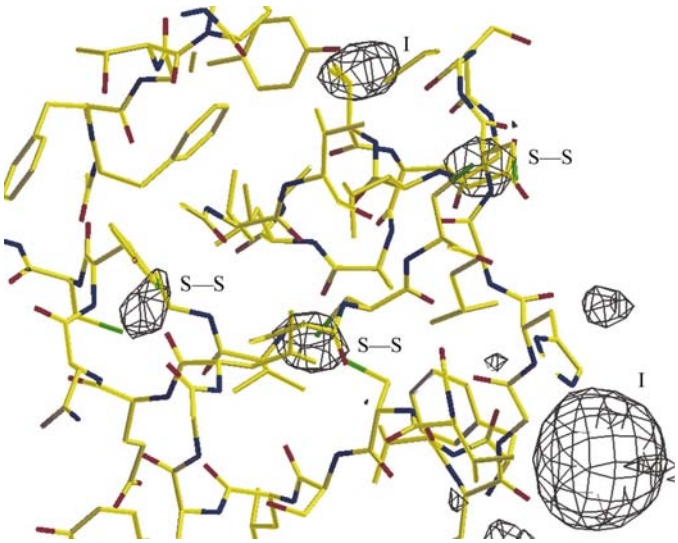

Figure 3
The anomalous difference electron-density map contoured at 2.5σ showing the signals of the S and I scattering atoms. Three peaks correspond to signals from the disulfide pairs and the other two peaks are identified as iodine signals.

scattering signal of iodine followed by solvent flattening. Three complete cycles of error filtering in both direct and reciprocal space to 3.0 Å (1402 anomalous reflections) were performed to screen for chemically reasonable structural fragments from preliminary maps as well as for strong reflections or weighting structure factors determined by their figures of merit. The enantiomorph ambiguity test shows that the enatiomer coordinates were in the right-hand orientation with an average figure of merit of 0.64 and a map inversion *R* factor of 0.45 (see Table 2). Subsequently, three phase extensions to 2.4 Å (1751 additional reflection) were applied in four cycles to obtain the phases. The final average figure of merit and the inverse map *R* factor for the 3153 reflections were 0.75 and 0.30, respectively. When the iodine signal was measured accurately, solvent flattening was an effective means of estimating the protein phases. Consequently, electron-density maps suitable for atomic fitting were obtained using phase information from the two I atoms.

Since the data set was of high redundancy, the sulfur signals were also detected and the sulfur positions determined from the anomalous difference Fourier map. The *ISAS* procedure was applied as described above using the signals of the two previously identified I atoms with the three additional sulfur signals. The *ISAS* data statistics showed only slight improvement, indicating that in this particular case the iodine derivatives were sufficient to provide adequate signals for phase determination (Table 2).

Table 2
ISAS data statistics.

Phasing from iodine signals.

	Figure of merit	*R* (inverse map)	Correlation coefficient
Initial	0.64	0.449	0.858
Final	0.75	0.296	0.945

Phasing from iodine and sulfur signals.

	Figure of merit	*R* (inverse map)	Correlation coefficient
Initial	0.70	0.408	0.886
Final	0.79	0.276	0.952

Two sections of an experimental *ISAS* electron-density map at 2.4 Å resolution are shown in Fig. 4, illustrating the quality of the iodine-phasing results. An α-helix backbone is traced (orange tracing) against the experimental electron density and is overlapped with the refined coordinates of the C^{α} helical

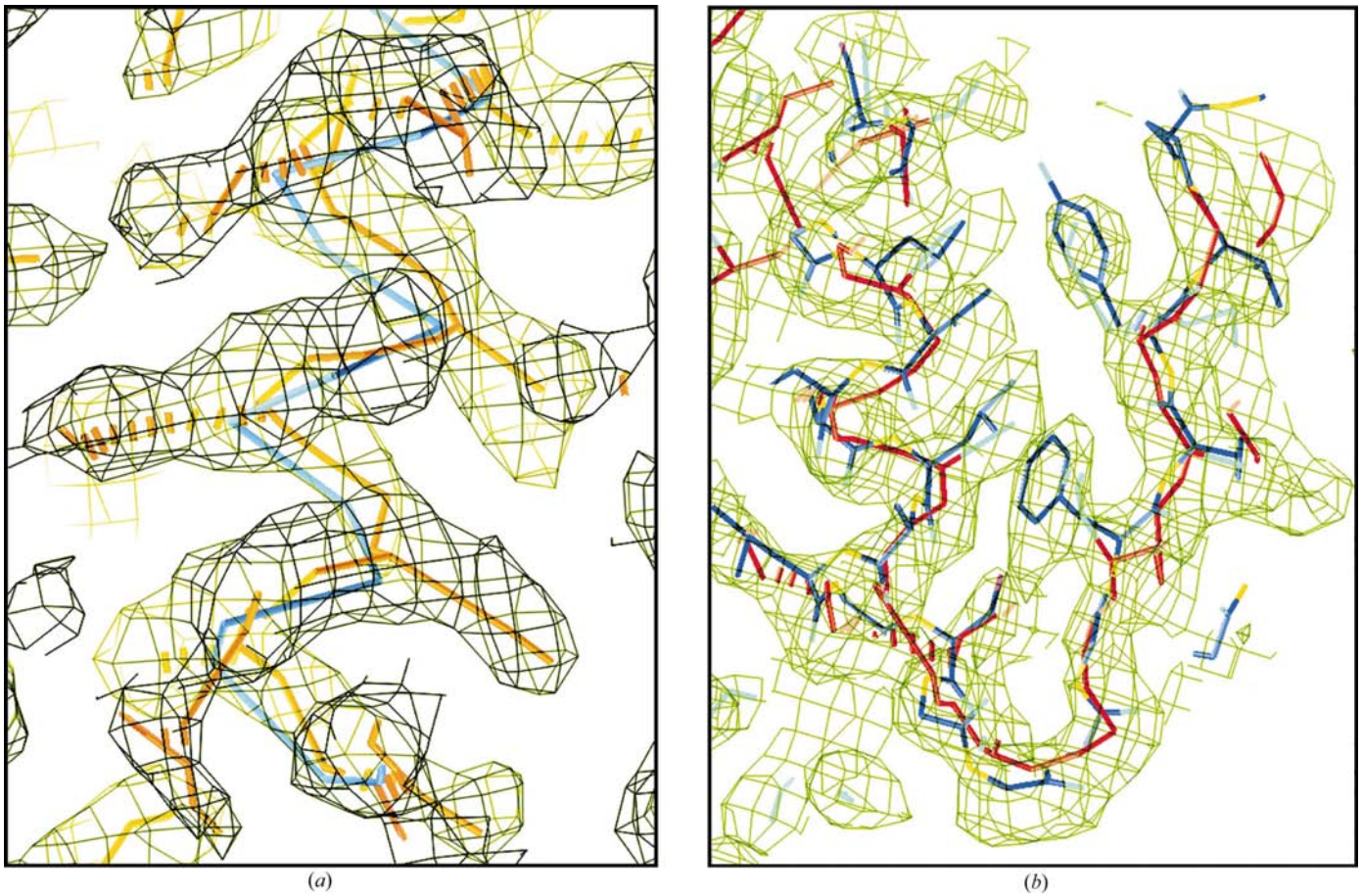

Figure 4
Experimental *ISAS* electron-density maps at 2.4 Å resolution. (*a*) shows a C^{α} helical backbone (orange) traced against the experimental density. The refined coordinates of insulin obtained from the Protein Data Bank (PDB code 1bph) were overlaid (blue) on the experimental tracing. Similarly, (*b*) shows the density outlined with the experimental C^{α} backbone (orange-red) superimposed with the PDB structure (blue) with its side chains in a loop region. The experimental structure has very high correlation with the known structure, indicative of the high quality of the iodine-phasing results.

tracing (positions Cys7–Leu17) from the Protein Data Bank (Berman *et al.*, 2000; PDB code 1bph) insulin structure (Fig. 4*a*). Fig. 4(*b*) illustrates a loop region corresponding to amino acids Cys7–Pro28 of the insulin PDB structure. A C^{α} backbone traced against the experimental density is compared with the overlaid coordinates of the known insulin structure. The initial structure correlates very well with the known structure, confirming the accuracy of the *ab initio* experimental phase determination. At the crystallographic level, we made no effort to execute any further refinement, as the purpose of this study is to obtain a traceable electron-density map for an initial model.

4. Conclusions

In the crystal-growth component, it is very practical for this procedure to be exploited in a matrix screening, where a range of different salts can be used to screen proteins in individual capillaries. This arrangement thereby provides a three-dimensional array where selection is based on two variables (such as salt type or pH) *versus* self-formed supersaturated concentrations of precipitation reagents. In the case of high-throughput applications, the goal is to screen for large numbers of protein types, common cryo-reagents and strong scattering atoms (halides or heavy metals) which can be easily incorporated in the screening process as described in this paper.

The present structural genomic projects endeavor to crystallize as many proteins as can be produced by recombinant overexpression systems, screen for suitable crystals for X-ray analysis and to perform rapid structure determination. This implementation of the counter-diffusion technique linked to the advancement of current crystallography software is a powerful structure-determination method that consolidates three principal steps (crystal growth, X-ray data collection and *ab initio* phase determination) into one for structure determination without crystal manipulation.

In our preliminary experiments, we have considered treating insulin as a total unknown protein without *a priori* knowledge of crystallization conditions. The insulin solution was prepared in a capillary, as described in this study, and equilibrated against the precipitating agents from Hampton Crystal Screen Kit I (Cat. HR2-110; Hampton Research, Laguna Niguel, CA, USA). Consequently, 50 capillaries were used to find *ab initio* crystallization conditions at room temperature that were observed within one week of equilibration. As a result, crystals were observed in capillaries corresponding to 20 conditions of the Hampton screen, of which 11 provided crystals suitable for X-ray diffraction. We are in the process of undergoing X-ray data collection and structure determination for the 11 conditions that produced diffracting crystals. The crystallization technique reported here is a potential tool for searching initial crystallization conditions followed by immediate X-ray diffraction analysis without any crystal handling.

The ease of collection and processing of X-ray data is truly limited by the quality of the crystal. The counter-diffusion geometry allows the equilibration process to be mediated by the formation of a supersaturation gradient. Therefore, the likelihood of finding an optimal crystal for structure determination is very favorable in this configuration. In addition, the incorporation of any additives is controlled by diffusion mass transport so that stress and damage imposed on the crystals are minimized.

Once a suitable crystal for X-ray diffraction is obtained, the crystallographic bottleneck step is the accurate determination of an *ab initio* phase. The *ISAS* procedure (Liu *et al.*, 2000; Wang, 1985) is a combined software package to rapidly determine phase information from anomalous signals and calculate an initial electron-density map. Different crystallographic software packages have been used for fast phase calculations using anomalous signals. In our case, the combination of *XTALVIEW*, *PHASES* and the *CCP*4 package was the easiest for the calculation and refinement of the anomalous scattering-atom position to be used in *ISAS* to produce a suitable electron-density map for initial modeling. The crystallographic calculations performed with a complete data set required less than 3 h. The whole process for phase determination is rapid once crystals are obtained. In the case of insulin, the entire procedure from the crystal growth to the first initial experimental electron-density map calculation for tracing and refinement took less than four weeks. Most of the time was consumed by the equilibration period during crystal growth and the home-source data collection. Even though this process does not appear to be strikingly fast, we demonstrate the technique to be competitive with traditional optimization methods for crystal growth, cryogenic soaking, incorporation of an atom useful for phasing, data collection and the determination of an initial model.

We are in the process of automating the methodology described here where a large number of proteins can be screened for crystallization in capillaries and those that contain crystals can undergo *in situ* X-ray analysis for structure determination.

We express our gratitude to Drs Zhi-Jie Liu and B. C. Wang for their valuable assistance and guidance in the final crystallographic analysis for the usage of the *ISAS* crystallography package. We also thank Dr Edward Meehan for his helpful discussion, Dr Liqing Chen for his assistance with the X-ray facility and Joyce Looger for her help in the software installations. This work was supported by NASA, Alabama Structural Biology Consortium NSF-EPSCoR and the NIH Structural Genomics project.

References

Berman, H. M., Westbrook, J., Feng, Z., Gilliland, G., Bhat, T. N., Weissig, H., Shindyalov, I. N. & Bourne, P. E. (2000). *Nucleic Acids Res.* **28**, 235–242.

Blundell, T. L. & Johnson, L. N. (1976). *Protein Crystallography.* London: Academic Press.

Chen, L., Rose, J. P., Breslow, E., Yang, D., Chang, W. R., Furey, W. F., Sax, M. & Wang, B.-C. (1991). *Proc. Natl Acad. Sci. USA*, **88**, 4240–4244.

Collaborative Computational Project, Number 4 (1994). *Acta Cryst.* D**50**, 760–763.
Dauter, Z. & Dauter, M. (1999). *J. Mol. Biol.* **289**, 93–101.
Dauter, Z., Dauter, M. & Rajashankar, K. R. (2000). *Acta Cryst.* D**56**, 232–237.
Dauter, Z., Li, M. & Wlodawer, A. (2001). *Acta Cryst.* D**57**, 239–249.
Dodson, E. J., Dodson, G. G., Lewitova, A. & Sabesan, M. (1978). *J. Mol. Biol.* **125**, 387–396.
Ducruix, A. & Giegé, R. (1999). *Crystallization of Protein and Nucleic Acids, a Practical Approach*, 2nd ed. Oxford: IRL Press.
Fasman, G. D. (1989). *Practical Handbook of Biochemistry and Molecular Biology.* Boca Raton, Florida: CRC Press.
Furey, W. & Swaminathan, S. (1997). *Methods Enzymol.* **277**, 590–620.
García-Ruiz, J. M. (1991). *Key Eng. Mater.* **58**, 87–106.
García-Ruiz, J. M. & Moreno, A. (1994). *Acta Cryst.* D**50**, 484–490.
García-Ruiz, J. M. & Moreno, A. (1997). *J. Cryst. Growth*, **178**, 393–401.
García-Ruiz, J. M., Moreno, A., Otálora, F., Viedma, C., Rondón, D. & Zautscher, F. (1998). *J. Chem. Ed.* **75**, 442–446.
García-Ruiz, J. M., Novella, M. L., Moreno, R. & Gavira, J. A. (2001). *J. Cryst. Growth*, **232**, 165–172.
García-Ruiz, J. M., Otálora, F., Novella, M. L., Gavira, J. A., Sauter, C. & Vidal, O. (2001). *J. Cryst. Growth*, **232**, 149–155.
Garman, E. F. & Schneider, T. R. (1997). *J. Appl. Cryst.* **30**, 211–237.
Gavira, J. A. (2000). PhD thesis. University of Granada, Spain.
Green, D. W., Ingram, V. M. & Perutz, M. F. (1954). *Proc. R. Soc. London A*, **40**, 287–307.
Harding, M. M., Hodgkin, D. C., Kennedy, A. F., O'Conner, A. & Weitzmann, P. D. J. (1966). *J. Mol. Biol.* **16**, 212–226.
Harker, D. (1956). *Acta Cryst.* **9**, 1–9.
Hendrickson, W. A. (1985). *Trans. Am. Crystallogr. Assoc.* **21**, 11–21.
Hendrickson, W. A. & Teeter, M. M. (1981). *Nature (London)*, **290**, 107–113.
Kleywegt, G. J. & Jones, T. A. (1997). *Methods Enzymol.* **277**, 525–545.
Lim, K., Nadarajah, A., Forsythe, E. L. & Pusey, M. L. (1998). *Acta Cryst.* D**54**, 899–904.
Liu, Z.-J., Vysotski, E. S., Chen, C.-J., Rose, J. P., Lee, J. & Wang, B.-C. (2000). *Protein Sci.* **9**, 2085–2093.
Lopéz-Jaramillo, F. J., García-Ruiz, J. M., Gavira, J. A. & Otálora, F. (2001). *J. Appl. Cryst.* **34**, 365–370.
Lopéz-Jaramillo, F. J., Moraleda, A. B., Gonzalez-Ramirez, L. A., Carazo, A. & García-Ruiz, J. M. (2002). *Acta Cryst.* D**58**, 209–214.
McPherson, A. (1999). *Crystallization of Biological Macromolecules.* New York: John Wiley & Sons.
McRee, D. E. (1999). *Practical Protein Crystallography*, 2nd ed. San Diego: Academic Press.
Otwinowski, Z. & Minor, W. (1997). *Methods Enzymol.* **276**, 307–326.
Smith, J. L. & Hendrickson, W. A. (1983). *Nature (London)*, **303**, 86–88.
Vidal, O., Robert, M. C. & Boué, F. (1998). *J. Cryst. Growth*, **190**, 257–270.
Wang, B.-C. (1985). *Methods Enzymol.* **115**, 90–112.